

# Investigation of ordered proton beams at S-LSR

*A. Noda, T. Shirai, H. Souda, H. Tongu*

Institute for Chemical Research, Kyoto University, Uji-City, Kyoto 611-0011, Japan

*I.Meshkov, A.Sidorin, A.Smirnov*

Joint Institute for Nuclear research, Dubna 141980, Russia

*K.Noda*

National Institute of Radiological Sciences, Inage, Chiba 263-8555, Japan

*M.Grieser*

Max Planck Institute for Nuclear Physics, 69177 Heidelberg, Germany

## Introduction

Since the very low momentum spread for proton beam was reached at NAP-M experiments [1] the ordered ion beams were observed at storage rings ESR [2], SIS [3] (GSI, Darmstadt), CRYRING [4] (MSL, Stockholm). At the storage ring TSR (MPI, Heidelberg) an indication of an ordering state was found for a  $^{32}\text{S}^{16+}$  beam [5]. A few attempts for the ordering formation were made on the storage ring COSY [6] (FZJ, Juelich). Recently the ordered proton beam was observed on S-LSR [7] (Kyoto University).

This article presents theoretical and experimental investigations of proton beams at S-LSR which have the aim to formulate the necessary conditions for the achievement of the ordering state. The simulation of the ordered state and the beam evolution during cooling process was done with the BETACOOOL code [8].

Initially the ordered state of ion beams was observed at ESR for heavy ions only [9]. For light ions  $\text{C}^{6+}$ ,  $\text{Ne}^{10+}$ ,  $\text{Ti}^{22+}$  the sudden reduction of momentum spread with decreasing particle number was not measured. Later the ordered state was reached for light ions (except protons) [10]. From analysis of the ESR experimental results we can assume that the ordered state can be observed if the dependence of momentum spread on particle number  $\Delta P/P = \alpha N^\xi$  has a power coefficient  $\xi \leq 0.3$ .

This condition is in good agreement with COSY [6] and NAP-M [1] experiment where  $\xi \geq 0.5$  and a sudden reduction of the momentum spread was not observed. The same situation was at S-LSR one year ago when  $\xi$  had a value about 0.4 and the ordered state was not observed.

The experimental and theoretical results which are presented in this article were done for the dependence of the momentum spread and transverse emittances on particle number with different misalignments of magnetic field at the cooler section. Mainly all simulations were done with the Model Beam algorithm in the BETACOOOL program.

## 1. S-LSR setup

S-LSR is a compact storage/cooler ring with the circumference of 22.557 m. The ion beam was a 7 MeV proton beam, cooled by the electron beam cooler. The measured beam parameters were a momentum spread and a horizontal beam profile. They were measured by a Schottky monitor and a residual gas ionization monitor, respectively. The particle number in the ring was measured by the residual gas ionization monitor and a bunch intensity monitor.

The parameters of the proton beam and the electron cooler are shown in Table 1. Fig.1 shows the view of S-LSR and Fig.2 shows the lattice parameters of one period.

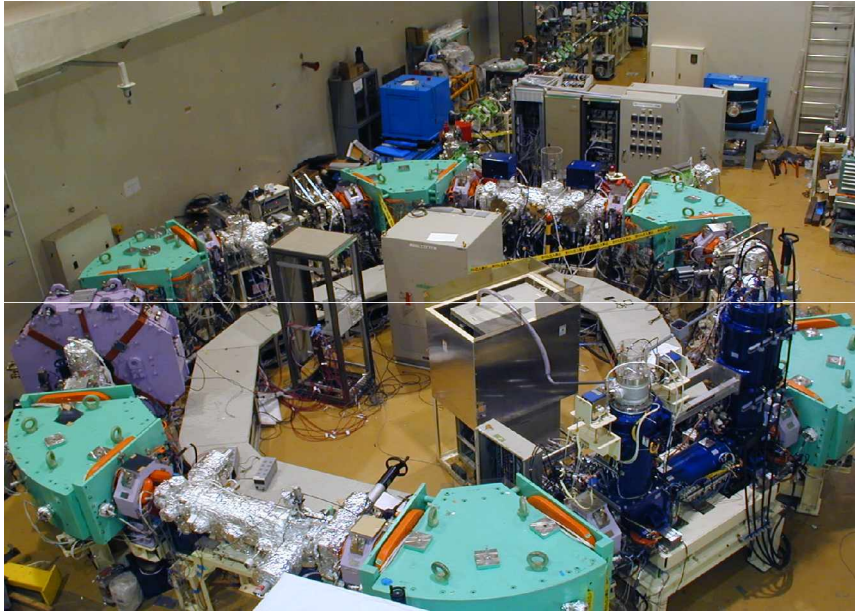


Fig.1 Photograph of S-LSR.

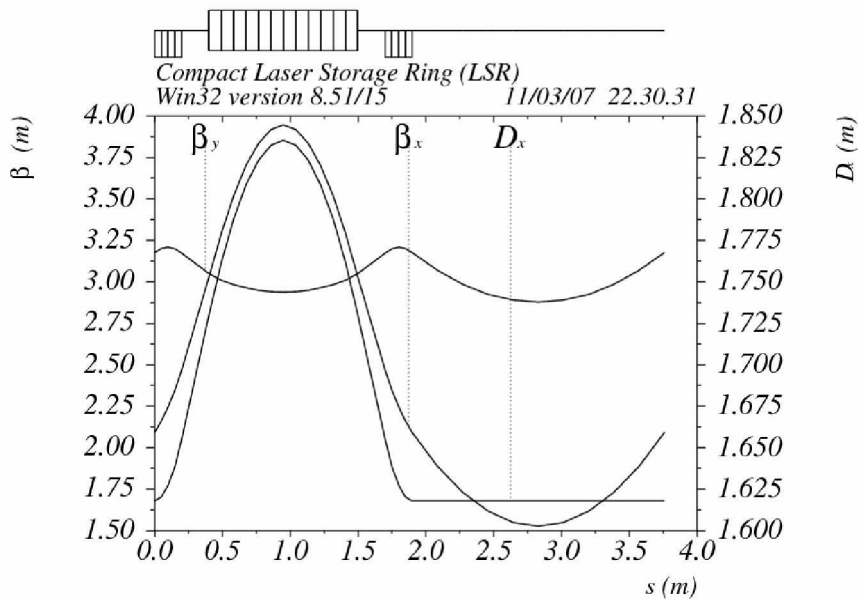


Fig.2. The lattice parameters of one period.

Table 1. S-LSR experimental parameters of the proton beam and the electron cooler

<b>Proton Beam</b>	
Proton Energy	7 MeV
Revolution Frequency	1.61 MHz
Betatron Tune	(1.645, 1.207)
Vacuum Pressure (in Ave.)	$6 \times 10^{-9}$ Pa
<b>Electron Cooler</b>	
Electron Current	25.5 mA or 102 mA
Electron Density	$2.2 \times 10^6$ e <sup>-</sup> /cm <sup>3</sup> or $8.8 \times 10^6$ e <sup>-</sup> /cm <sup>3</sup>
Electron Energy	3.8 keV
Electron Beam Radius	25 mm
Magnetic Field of Solenoid	500 Gauss
Magnetic Expansion Factor	3
Vacuum Pressure (at EC)	$4 \times 10^{-9}$ Pa

## 2. Field error and formation of misalignments in cooler solenoid

For the investigation of the dependence of the momentum spread on the particle number a misalignment of the magnetic field at the cooler solenoid was proposed. The field error was created by the Helmholtz coil and it gives a uniform transverse field over the cooler solenoid. In order to reproduce a more realistic field error, the zigzag field can be formed by the vertical correction coils. Fig.3 shows an example of the zigzag field, where the vertical component of the magnetic field are presented. The blue line presents the normal vertical component of the magnetic field. The red line shows the measured filed data, when HR2=HR3=2.2A. The vertical field of 0.5 Gauss corresponds to the field inclination of 1 mrad.

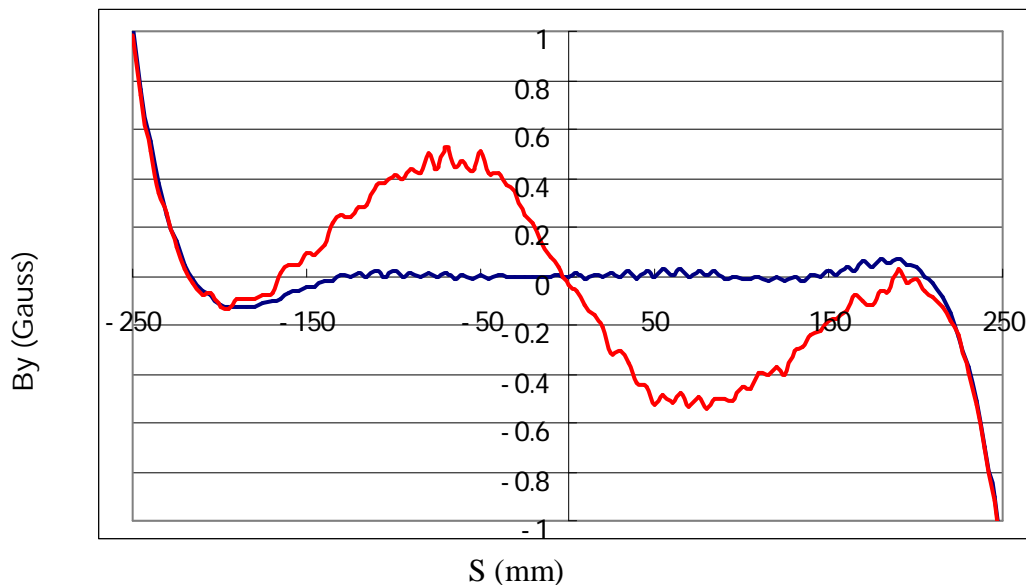


Fig.3. Vertical component of the magnetic field in the cooler solenoid coil. The blue line is the present field. The red line is the zigzag field created by the correction coils.

### 3. Magnetic field misalignment at the cooler section

To heat the ion beam the different angle between the electron beam and ion beam were chosen, affecting the Schottky spectra shown in Fig.4. The Schottky spectrums were measured for particle number of  $3 \times 10^7$  and an electron current of 102 mA. The left Spectrum was measured without a misalignment, in the right one in Fig.4, a horizontal misalignment of 2 mrad was chosen. It can be seen that some of the protons did not captured at the high energy side if the misalignment is 2 mrad.

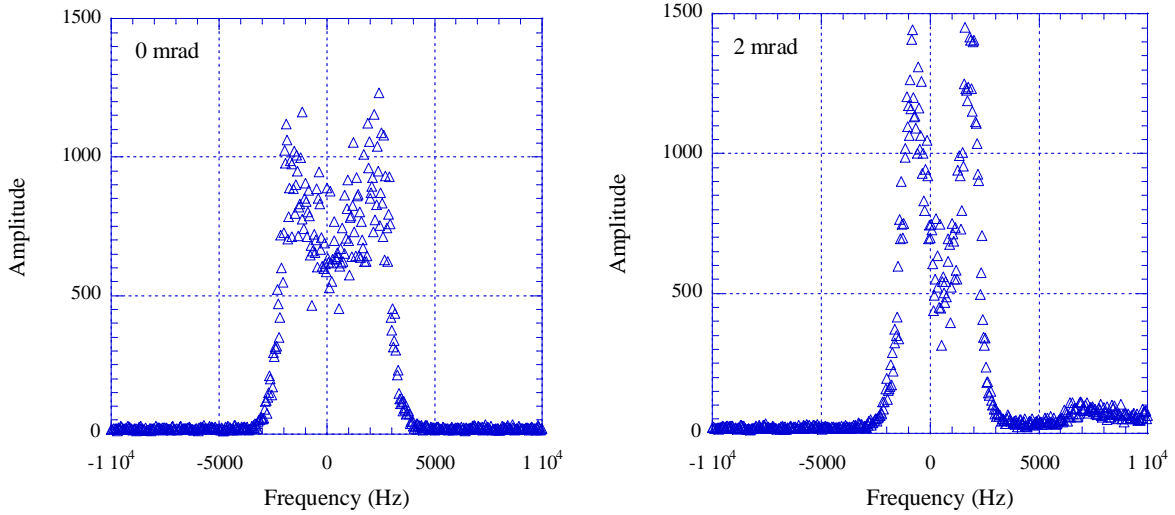


Fig.4. Schottky spectrums with the particle number of  $3 \times 10^7$  and the electron current of 102 mA. The misalignment angles are 0 and +2 mrad.

Simulation with the BETACOOOL program shows (Fig.5,a) that the longitudinal profile has a nonsymmetrical shape and some particles are distributed in long tail caused by the influence of space charge parabola of the electron beam (Fig.6,a).

The horizontal profile has a very specific shape (Fig.5,b) which is given by the horizontal misalignment of 2 mrad. It means that all particles are cooled to same horizontal angle and have the same invariant in the phase space (Fig.6,c).

This specific behavior of the transverse profiles which is known as Hopf bifurcation [11] was observed in first time in NAP-M experiments [12] and was used for measurement of the transverse cooling force at CRYRING [13]. The BETACOOOL simulation results are in good agreement with experimental one.

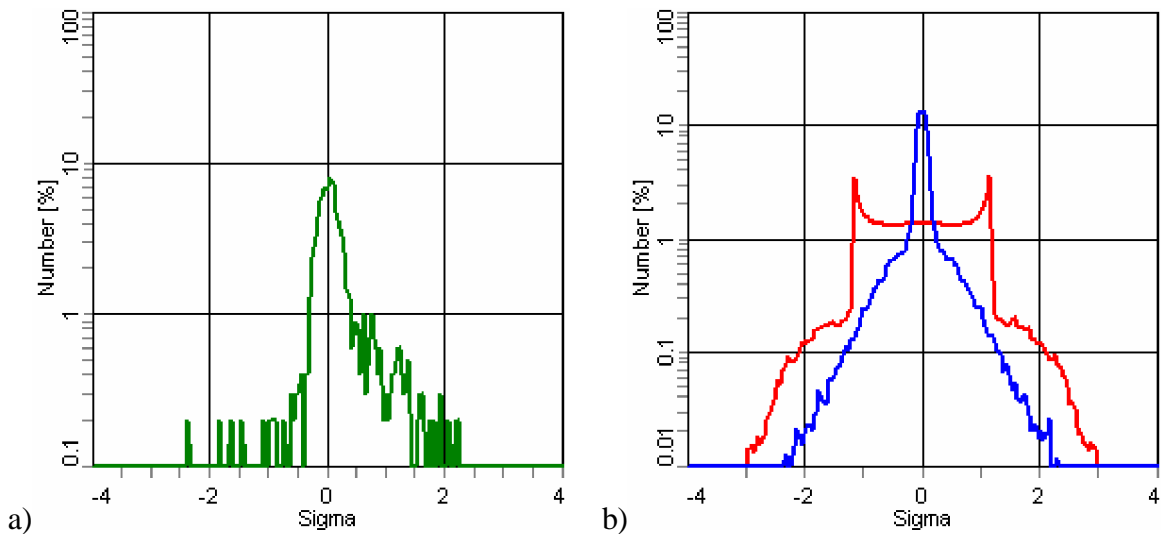


Fig.5. Simulation of momentum spread (a) and transverse profiles (b) for  $N_p=3 \times 10^7$ ,  $I_e=100\text{mA}$  and horizontal misalignment 2 mrad. Red line – horizontal profile, blue – vertical one.

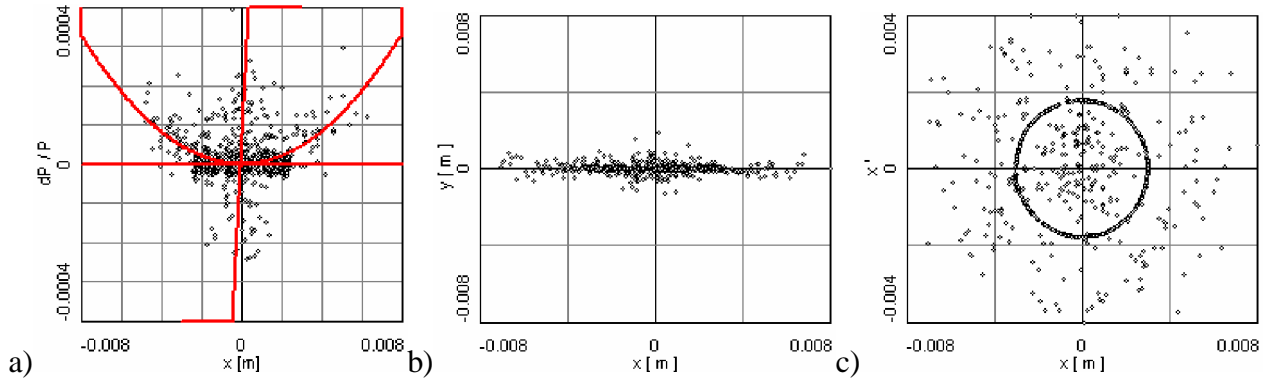


Fig.6. Distribution of model particle: momentum spread on horizontal coordinate (a), transverse profile (b), transverse phase space (c).  $N_p=3 \times 10^7$ ,  $I_e=100$  mA,  $M=2/0$  mrad (horizontal/vertical misalignment angle).

#### 4. Transverse profile measurement

The transverse profiles were measured by the ionization monitors with various misalignment angles (Fig.7). The electron current was 25.5 mA and 102 mA. The particle number was  $1 \times 10^7$  at the electron current of 25.5 mA and  $3 \times 10^7$  at 102 mA.

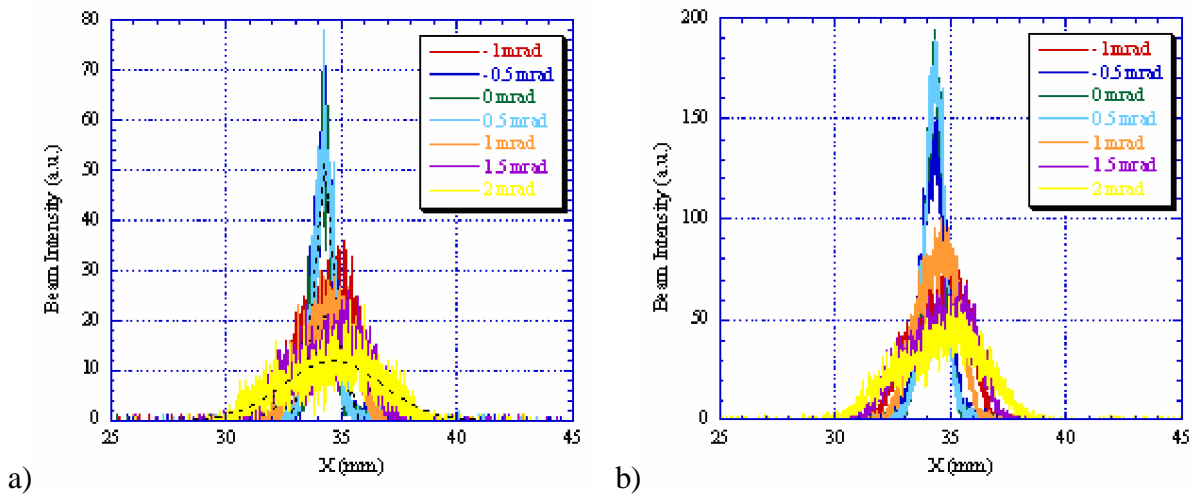


Fig.7. Transverse beam profiles measured by the ionization monitors. The electron current was 25.5 mA (a) and 102 mA (b). Horizontal misalignment angles  $M=-1, -0.5, 0, 0.5, 1, 1.5, 2$  mrad.

If the angle between electron and ion beam is increased the beam radius of the stored ion beam becomes larger as shown in Fig.8, where the radius is defined as the  $\sigma$  value of the Gaussian function fitting. The transverse size increases in accordance with misalignment angle. For some certain beam parameters (Fig.9,a) the measured transverse beam profile is in good agreement to the simulation result (Fig.5,b) when the transverse beam profile gets two peaks.

The transverse size of the proton beam does not depend on the particle number when the misalignment reaches a certain value (Fig.9,b). For large number of particles the transverse beam size is defined by intrabeam scattering.

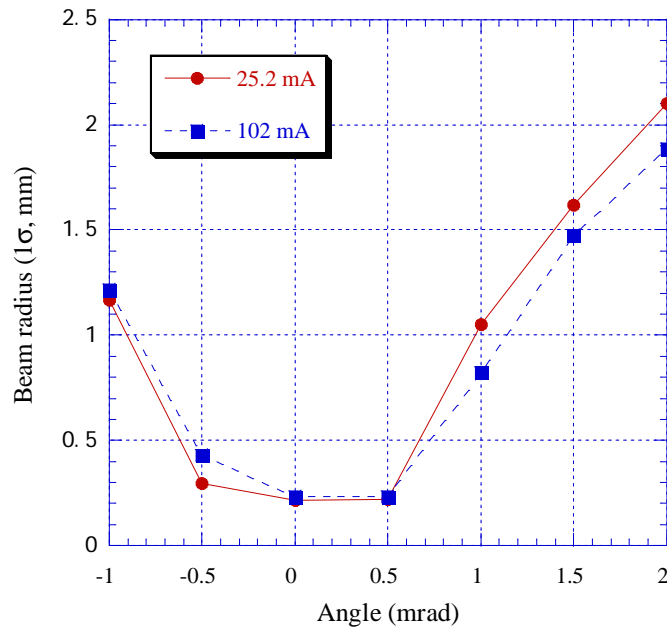


Fig.8. Transverse beam radius as a function of the misalignment angles, measured at two different electron currents. The particle number was  $1 \times 10^7$  (25.2 mA) and  $3 \times 10^7$  (102 mA)

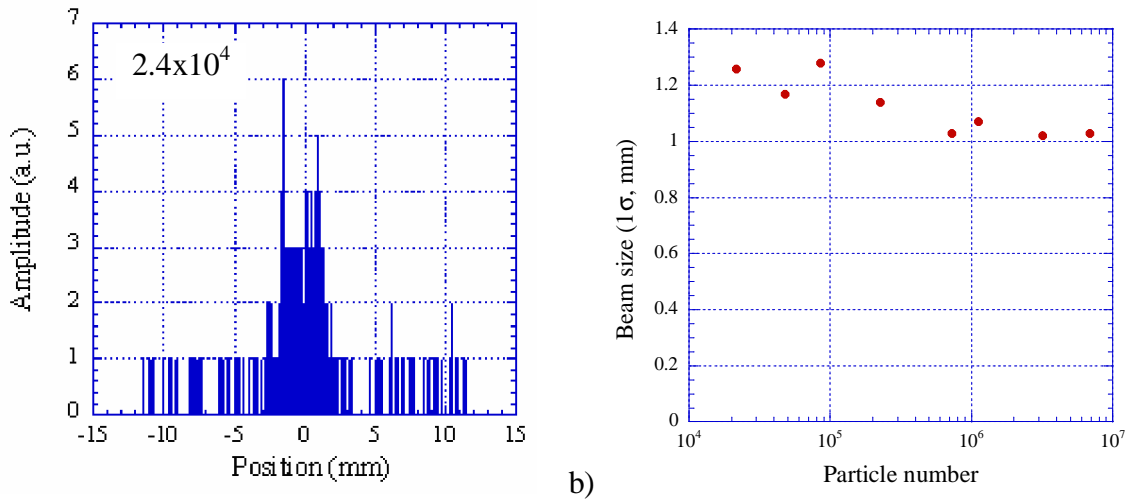


Fig.9. Transverse beam profile measured at a horizontal misalignment of 1 mrad (a) for  $N_p = 2.4 \times 10^4$  and transverse beam size as a function of the particle number (b).

## 5. Longitudinal cooling force measurement

Electron cooling force was measured with induction acceleration for a electron current of 50 mA and a proton current of  $0.1 \mu\text{A}$  (Fig.10,a). In the simulation the Parkhomchuk model [14] of the electron cooling force was used. The amplitude of the cooling force was fitted using a effective temperature (Fig.10,b) which corresponds to a solenoid field errors of about  $2 \times 10^{-5}$ .

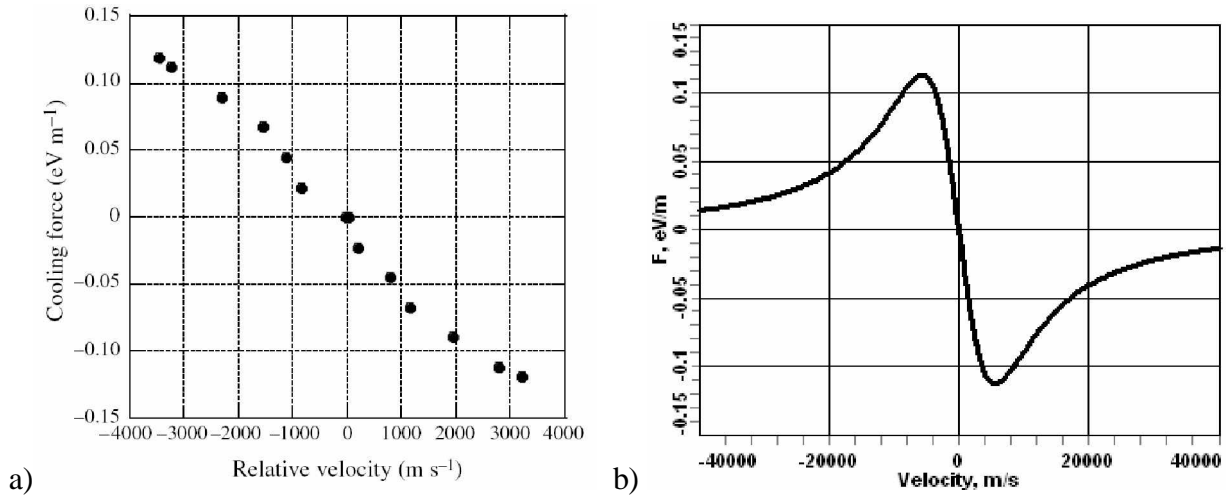


Fig.10. Measured longitudinal cooling force at an electron current of 50mA and ion current of  $0.1 \mu\text{A}$  using an induction accelerator (a), simulation results of the cooling force (b) for  $I_e=50 \text{ mA}$ ,  $T_{\perp}/T_{\parallel}=34/0.02 \text{ meV}$ .

The dependence of the maximum longitudinal cooling force on the horizontal misalignment angle was measured by the induction accelerator (Fig.11). The electron current was 25.5 mA.

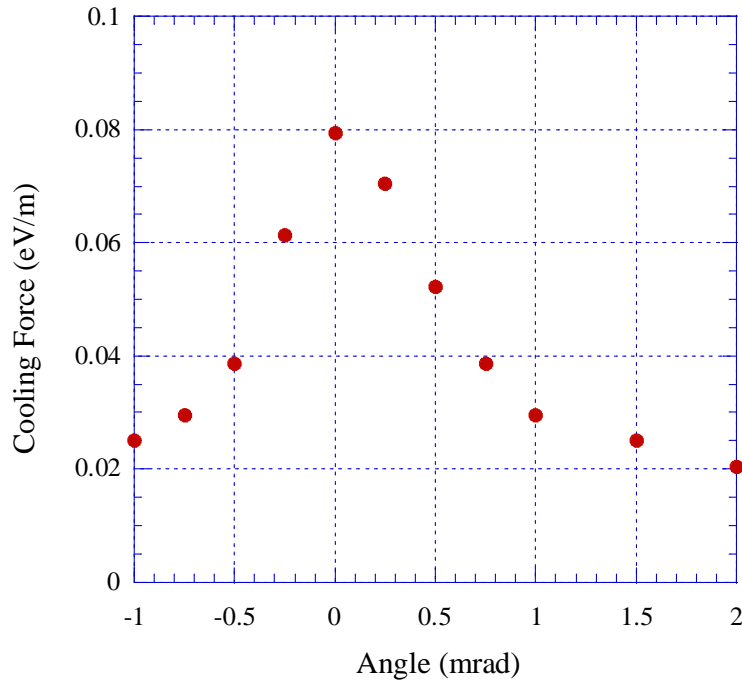


Fig.11. Maximum longitudinal cooling forces measured for different horizontal misalignment angles, using the induction accelerator. The electron current was 25.5 mA.

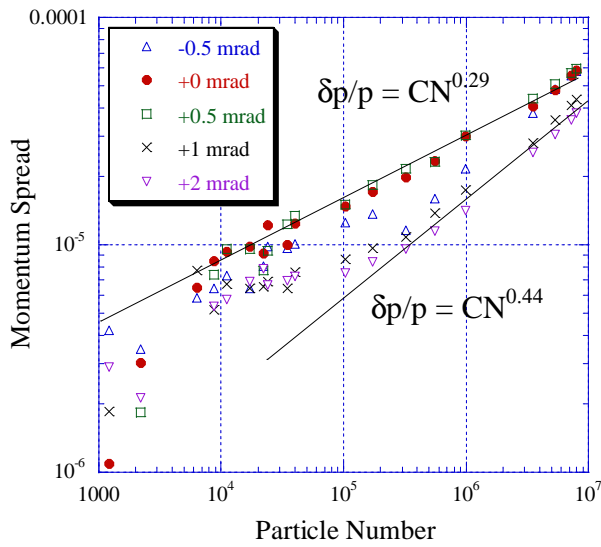
## 6. Experimental measurements of momentum spread on particle number

The momentum spread at different misalignment angles of the electron beam was measured. The results are summarized in Fig.12. The electron current was 25.5 mA in Fig.12 (a), (c), (d) and 102 mA in Fig.12 (b). In Fig.2 (a), (b) a horizontal misalignment, in Fig.12 (c) a vertical one and in Fig.12 (d) a horizontal and vertical were chosen. At first, an electron beam alignment was done to maximize the longitudinal cooling force measured by the induction accelerator. This setting was defined as “0 mrad”. Then, the misalignment between the electron and proton beams was created by the Helmholtz coils in the horizontal and vertical directions. The misalignment angles were -0.5, 0, 0.5, 1, 2 mrad.

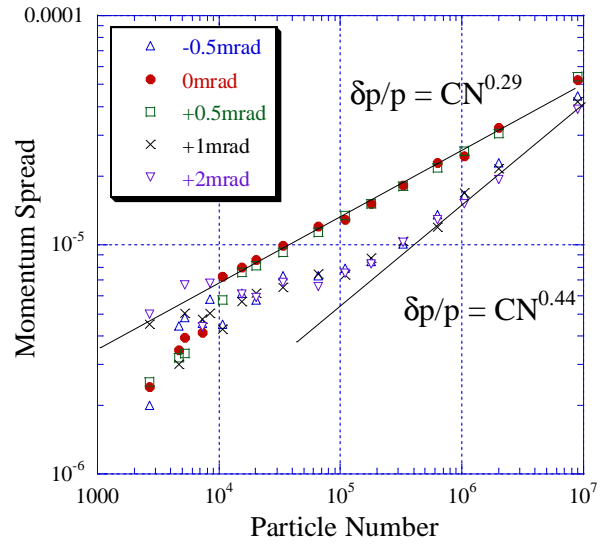
For small alignment error ( $<0.5$  mrad), the momentum spread was proportional to  $N_p^{0.29}$ . When the alignment error was larger ( $>0.5$  mrad), the momentum spread scaled with  $N_p^{0.44}$  at large particle number and saturated (or changed the slope) below  $3 \times 10^5$  particles. A similar behavior was observed in all cases (Fig.12a-d). Especially, the behaviors at the horizontal and vertical misalignment were similar (see Fig.12a and Fig.12c). Using a misalignment in both directions, the momentum spread saturated at the larger momentum spread (see Fig.12d). The dependence of the momentum spread is similar to the results at COSY and NAP-M, while the particle number of NAP-M was different.

The drop of the momentum spread was observed at many horizontal or vertical misalignments, but it was not noticed in some cases. With large misalignments ( $>0.5$  mrad) in both directions, the drop of the momentum spread was not observed.

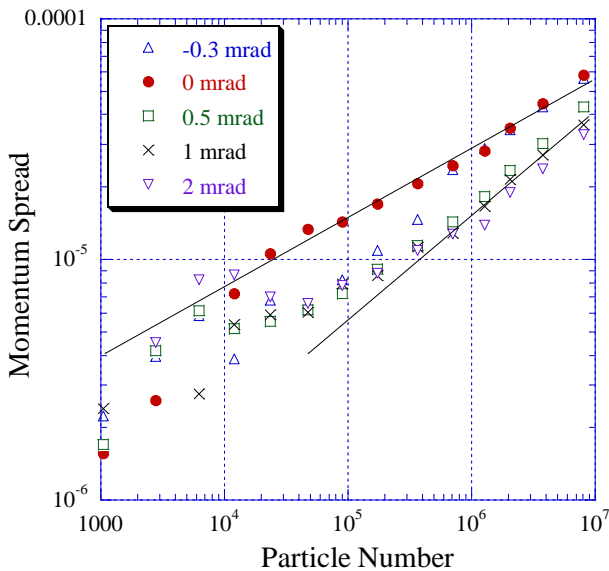
(a) : Horizontal misalignment with  $I_e=25.5$  mA



(b) : Horizontal misalignment with  $I_e=102$  mA



(c) : Vertical misalignment with  $I_e=25.5$  mA



(d) : Both misalignments with  $I_e=25.5$  mA

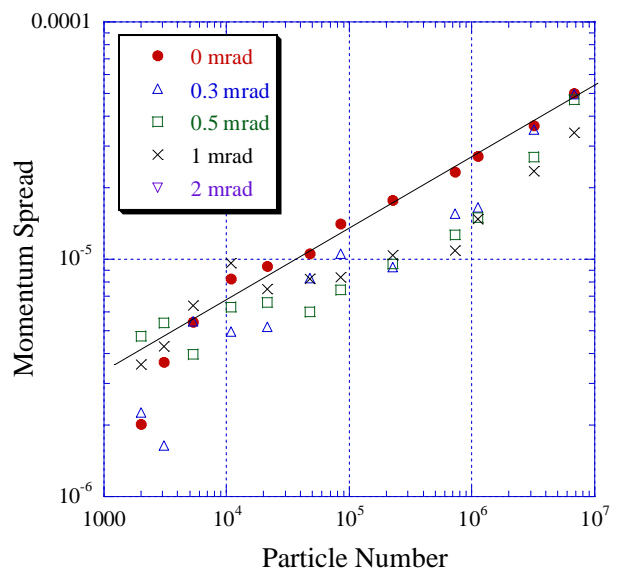
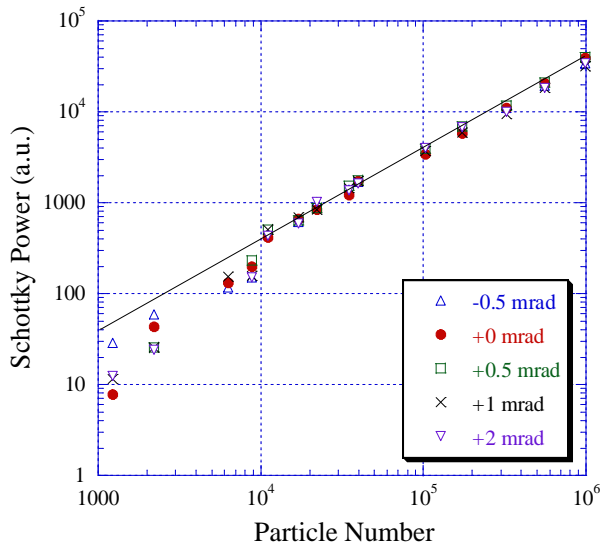


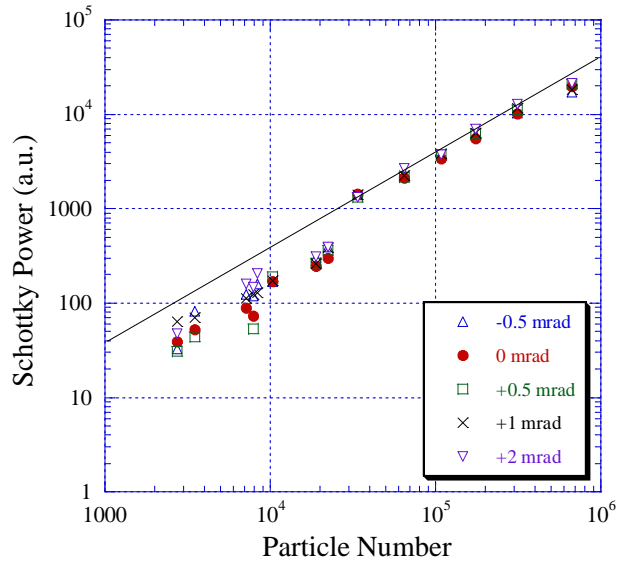
Fig.12 Momentum spread as a function of particle number for different misalignment angles. The electron current is 25.5 mA at (a), (c), (d) and 102 mA at (b). In (a), (b) a horizontal misalignment, in (c) a vertical and in (d) in both direction was chosen.

The Schottky powers as a function of the particle number are shown in Fig.13. The misalignment angles are the same as in Fig.12. The electron current was 25.5 mA in Fig.13 (a), (c), (d) and 102 mA in Fig.13 (b). In Fig.13 (a), (b) a horizontal misalignment, in Fig.13 (c) a vertical misalignment and in Fig.13 (d) in both directions was chosen. The solid line shows the function  $P_{\text{Schottky}}=0.04 \times N_p$  i(Fig.13a-d). The drop of the Schottky power was observed with a horizontal or vertical misalignment, but with a large misalignment angle ( $>0.5$  mrad) in the both directions, the drop of the Schottky monitor could not be observed.

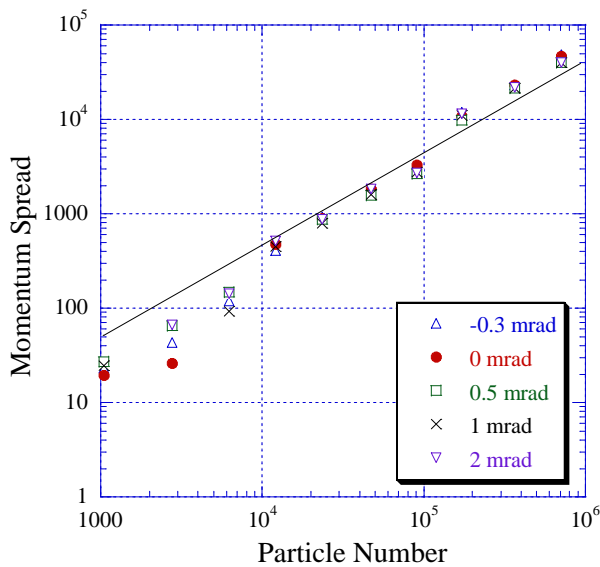
(a) : Horizontal misalignment with  $I_e=25.5$  mA



(b) : Horizontal misalignment with  $I_e=102$  mA



(c) : Vertical misalignment with  $I_e=25.5$  mA



(d) : Both misalignments with  $I_e=25.5$  mA

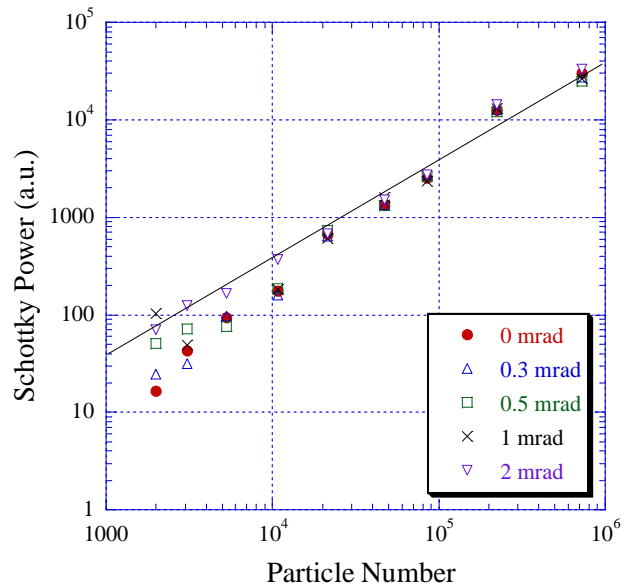


Fig.13 Schottky power as a function of particle number for different misalignment angles. The electron current is 25.5 mA at (a), (c), (d) and 102 mA at (b). The misalignment is the horizontal direction at (a), (b) and the vertical direction at (c) and both directions at (d). The solid line is  $P_{\text{Schottky}}=0.04 \times N_p$ .

We note the similarity between the data in February, 2006 (first measurement at S-LSR) and the data with the small misalignment in the both directions. The comparison is shown in Fig.14. This result suggests that the dependence of the momentum on the particle number in February, 2006 was determined by the electron beam misalignment in both directions. It is supposed that the drop of the momentum spread was prevented by the power supply ripples but it was not confirmed by the experiment.

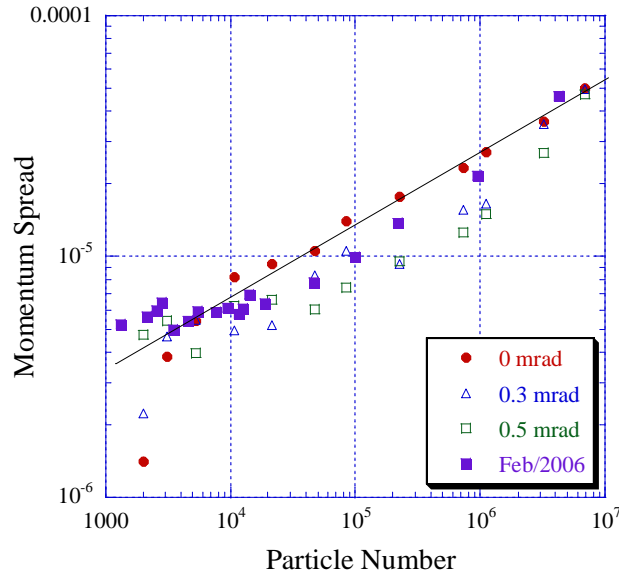


Fig.14. Comparison with the data in February, 2006 and the data with the misalignment in the both directions, which was subtracted from Fig.2 (d).

In the above measurements, the field error was created by the Helmholtz coils and they gave the uniform transverse field over the cooler solenoid. In order to simulate the more realistic field error, the zigzag field was formed by the vertical correction coils. Fig.3 shows an example of the zigzag field. In Fig.15 the momentum spread measured with and without zigzag field is compared. In both measurements the data are lying on the same line at particles numbers larger than  $10^4$ , whereas a jump in the momentum spread occurs at particle numbers between 1000 and 3000.

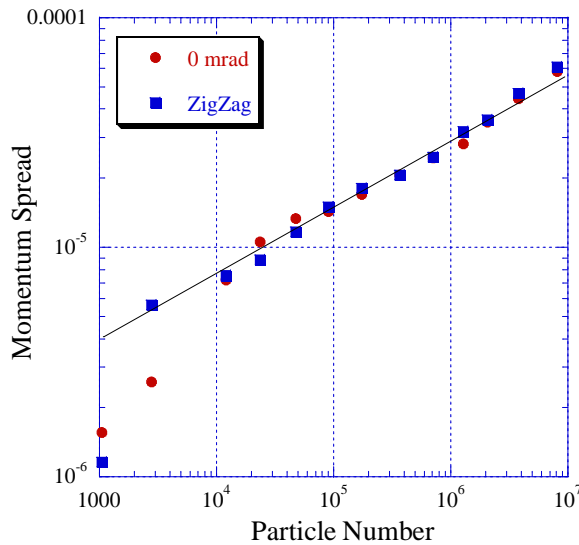


Fig.15. Measured momentum spread of a stored proton beam as a function of proton number. The blue marker corresponds to the normal field, and in the measurement described by the red markers a zigzag field, created by the vertical correction coils, was used.

## 7. Numerical simulation of the experimental data

The dependence of the momentum spread on the particle number for different misalignments was simulated with BETACOOOL code (Fig.16). The simulation shows that a transverse misalignment can change the power coefficient  $\xi$  in the range from 0.21 up to 0.53. In the case of a large horizontal misalignment only ( $M=1/0$ , 1/0.2 mrad) the power coefficient  $\xi$  can be changed up to values of about 0.45 and the ordered state can be reached (see Fig.16, 17). In the case of a large misalignment in both transverse direction ( $M=1/1$ , 2/2 mrad) the saturation of the momentum spread exist due large influence of the space charge parabola of the electron beam (Fig.17) and the ordered state can not be reached.

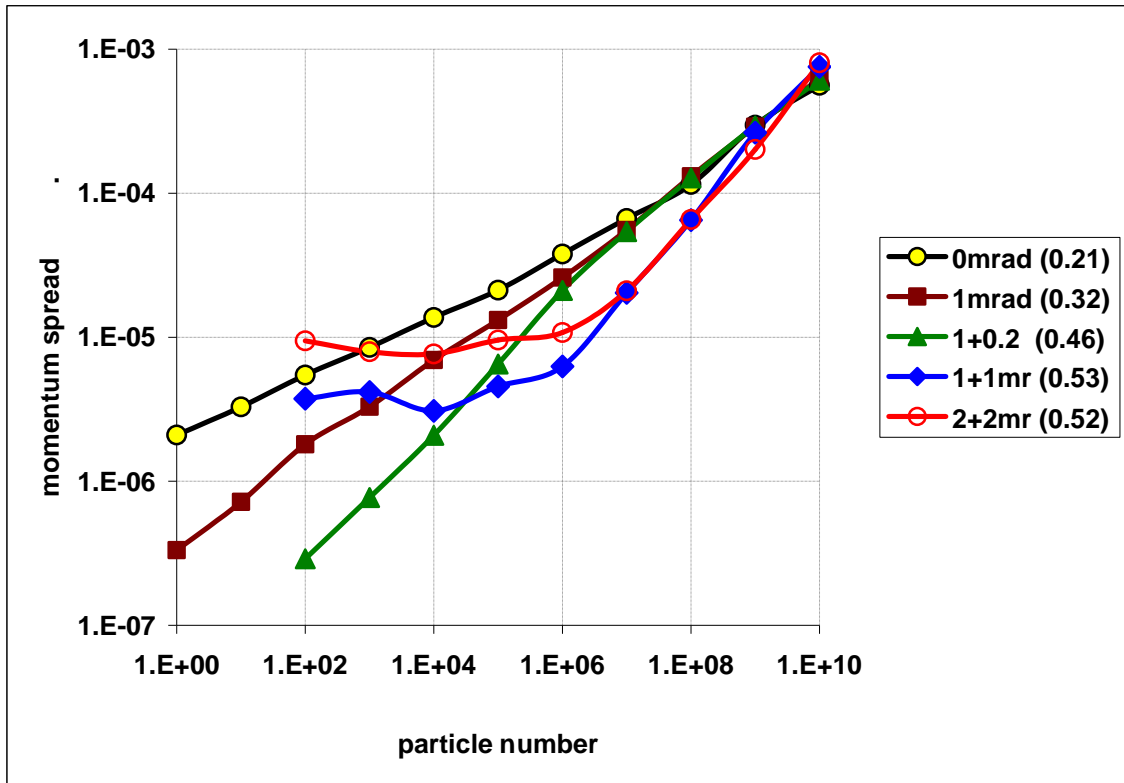


Fig.16. The dependence of the momentum spread on the particle number for different misalignments.  $I_e=25$  mA,  $M=0/0$ , 1/0, 1/0.2, 1/1 mrad,  $\xi=0.21$ , 0.32, 0.46, 0.53, 0.52.

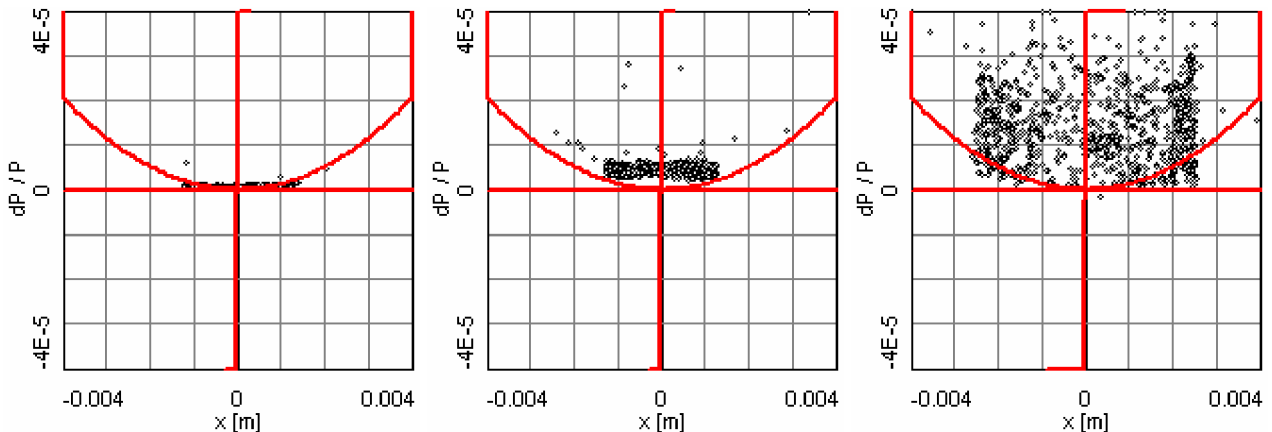


Fig.17. The particle distribution in the cooler section, points – model particles, red parabola describes the space charge parabola of the electron beam.  $I_e=25$  mA,  $N_p=100$ ,  $M=1/0.2$ , 1/1, 2/2 mrad.

## 8. Equilibrium between electron cooling and intrabeam scattering

The use of an additional field misalignment can change the power coefficient  $\xi$  but this behavior can not fully explain the difference of the  $\xi$  value measured in real experiments and predicted by the theory. Fig.18 describes intrabeam scattering and electron cooling at S-LSR, shown are intrabeam scattering rates and cooling rates for different momentum spreads and horizontal emittances. The summary diagrams in fig. 18 shows the horizontal and longitudinal equilibrium between IBS and electron cooling.

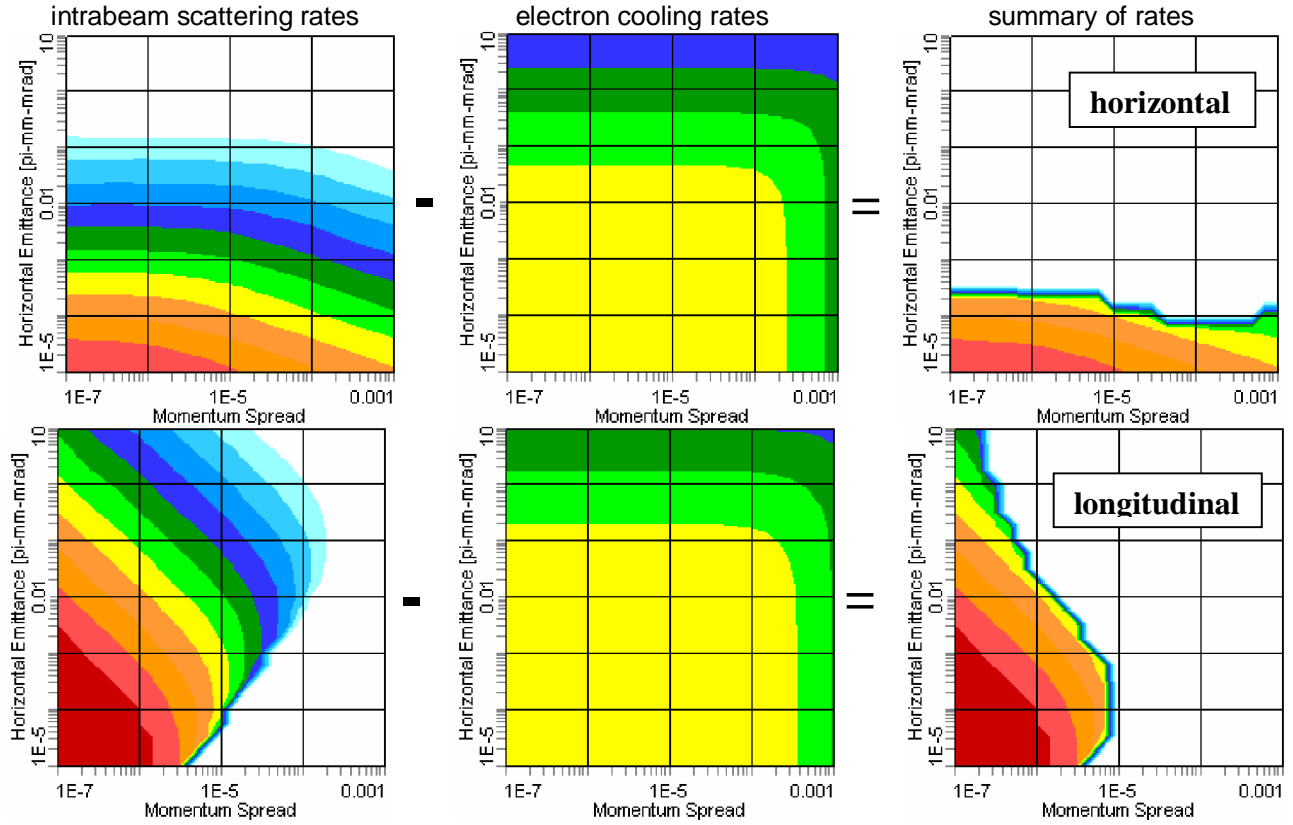


Fig.18. Intrabeam scattering rates (Martini model,  $N_p=10^3$ ) and electron cooling rates (Parkhomchuk model,  $I_e=25$  mA) for the S-LSR lattice structure. Each color corresponds to certain level of heating / cooling rates [1/sec], rate values are shown in Fig.19.

The experimental data as well the simulated beam evolution during the cooling process is presented in Fig.19. The simulation results for particle, without any misalignment, shows that the beam parameters cool down along the equilibrium of transverse and longitudinal temperature of the proton beam (Fig.19, red circles). The power coefficient in this case is  $\xi=0.21$  (Fig.16). The experimental results when the ordered state was observed (Fig.19, blue squares) show that the transverse temperature is much higher the longitudinal one and the power coefficient is  $\xi=0.29$  (Fig.12). But all these dependence can be described by parallel lines in the logarithmic plot (Fig.19).

The same behavior of the beam evolution during the cooling process was measured at the ESR when the transverse temperature is much higher then longitudinal one (Fig.20 [10], 21). Applying of some misalignment in the transverse direction increases the power coefficient  $\xi$ . But this additional transverse heating changes the behavior of the beam parameters in Fig.19 (green triangles). That means that the difference between experimental and theoretical behavior of beam parameters can not be explained by the misalignment or solenoid errors.

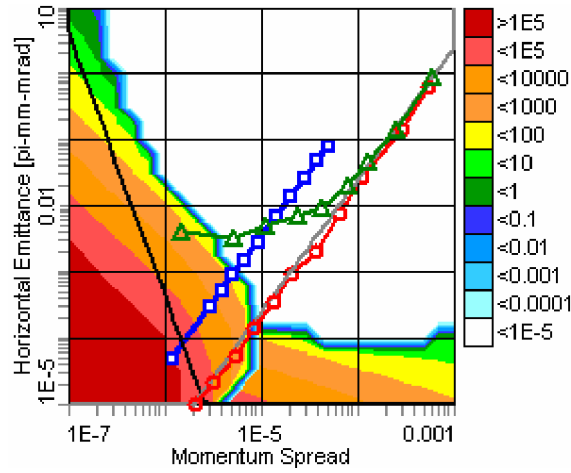


Fig.19. Overlap of horizontal and longitudinal sum of rates. **Gray line** –equilibrium of transverse and longitudinal temperature of proton beam, **black line** –  $\Gamma_2$  ordering criterion [15], blue square ( ) – experiment (line without point means drops to ordered state), red points (O) – simulation with zero misalignment, green triangle ( $\Delta$ ) – simulation with 0.2/0.2 mrad misalignment.

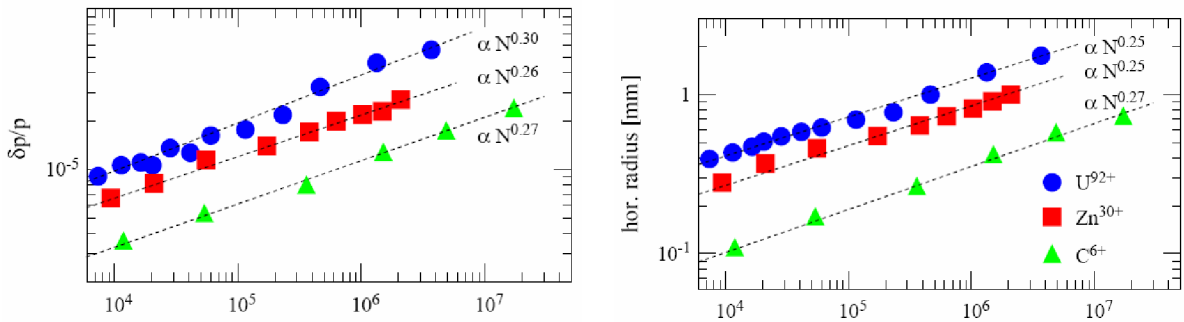


Fig.20. Dependence of momentum spread and horizontal size on particle number, measured at ESR.

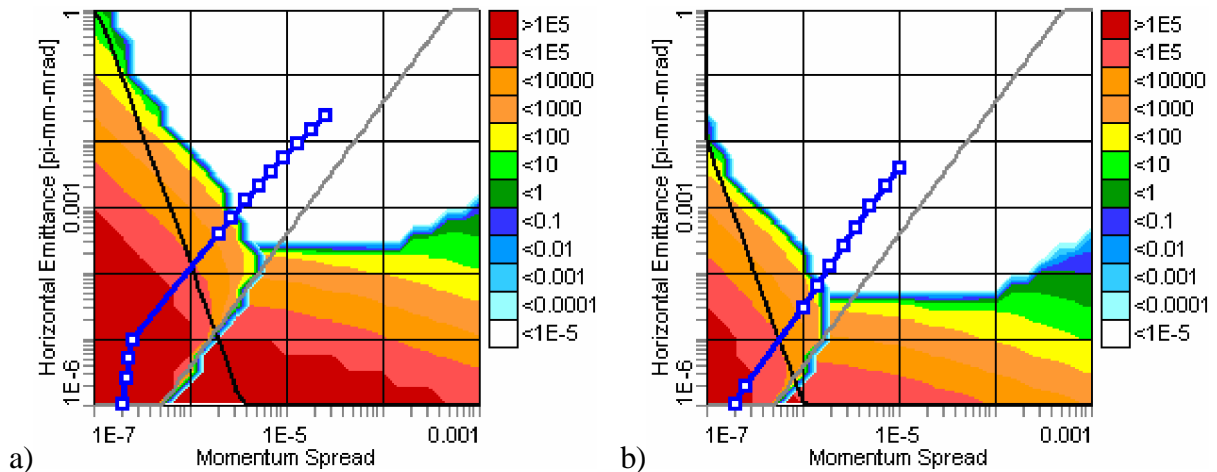


Fig.21. ESR experiment. Sum of ECOOL ( $I_e=250\text{mA}$ ) and IBS ( $N=10^3$ ) rates for  $\text{U}^{92+}$  (a) and  $\text{C}^{6+}$  (b), blue squares - experimental points taken from Fig.20.

Simulation with the Martini model shows that the value of the longitudinal component of the IBS heating rates before the sudden reduction of the momentum spread occurs is about  $10^3 \text{ sec}^{-1}$ , (Fig.19) which is one order larger than the electron cooling rates (Fig.18). Simulation with Molecular Dynamics technique shows that the IBS longitudinal component has some channel [6] with low value of heating rates (Fig.22,b).

This channel exists for the particle number up to  $5 \times 10^4$ . This channel disappears for a particle number larger than  $10^5$  what is closed to the transition point from string to zig-zag structure of crystalline beams [15]. IBS heating rates inside this channel for the small particle number is about  $50 \text{ sec}^{-1}$  which corresponds to the real electron cooling rates.

We can assume that the beam parameters go through this channel during the cooling process and the ordered state of the ion beam can be reached. It means that the specific experimental behavior of the cooling process when the transverse temperature of ion beam is much larger than the longitudinal ones helps us to reach the ordered state (Fig.17, 18).

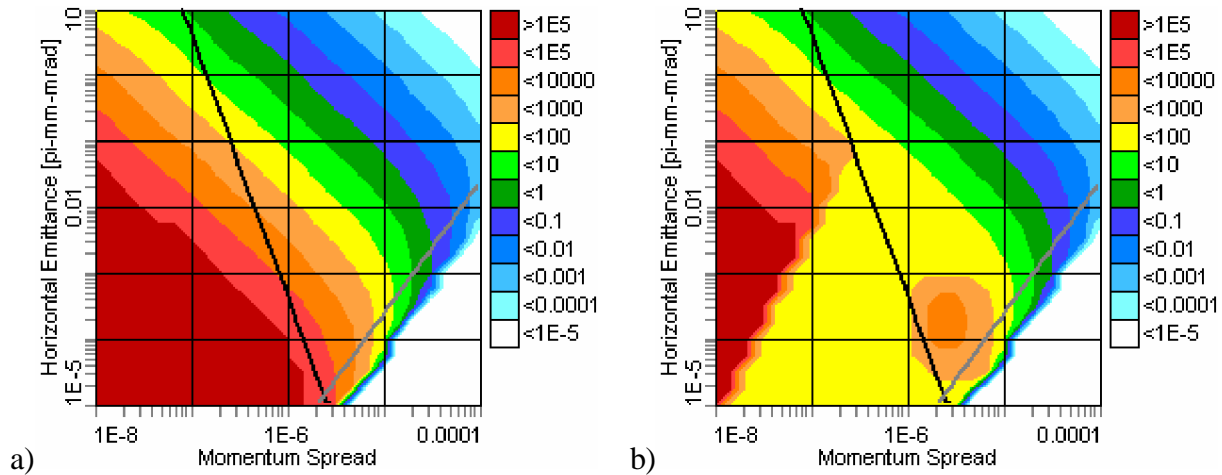


Fig.22. Intrabeam scattering rates for S-LSR lattice structure.  $N_p = 10^3$ .  
a) Martini model, b) estimation with Molecular Dynamics.

## Conclusion

In the normal experimental settings the ordered state can be reached for a power coefficient  $\xi \leq 0.3$ , describing the dependence of the momentum spread on the particle number. This value can be increased up to 0.45 with a special kind of magnetic field misalignment in one transverse direction only. In the case of a large field misalignment (or solenoid errors) in both transverse direction the power coefficient increases up to 0.53 and the ordered state of the ion beam can not be reached due to the large influence of the space charge parabola of the electron beam. This behavior of the momentum spread on the particle number can explain the experimental results where the power coefficient was  $\xi \geq 0.5$  and the ordered state was not observed.

In the experiments at ESR and S-LSR when the ordered state of ion beams was observed the transverse temperature was about one order larger than the longitudinal one and the power coefficient was in the range of  $\xi = 0.26-0.3$ . The theory of intrabeam scattering predicts that the power coefficient is  $\xi = 0.21$  for a coasting beam and the transverse and longitudinal temperature is equal during cooling process. These contradictions were not explained by the misalignment or solenoid errors of the magnetic field at the cooler section.

Simulation with the standard theory of IBS and Molecular Dynamics shows that the electron cooling force can not suppress the intrabeam scattering heating in the case of equal transverse and longitudinal temperatures of the ion beam. Probably in real experiments for the achievement of the ordered state the channel in the longitudinal component of IBS is used when the transverse temperature of ion beam is much larger than longitudinal one. The additional transverse heating with the field misalignment in one direction only does not destroy the ordered state and can be used for the investigation of the channel in the IBS longitudinal component.

## References

- [1] G.I.Budker, N.S.Dikansky, V.I.Kudelainen et al., Proc. 4th All-Union Conf. on Charged-Particle Accelerators [in Russian], Vol. 2 (Nauka, Moscow, 1975) 309; Part.Accel. 7 (1976) 197; At.Energ. 40 (1976) 49. E.Dementev, N.Dykansky, A Medvedko et al., Prep. CERN/PS/AA 79-41, Geneva (1979).
- [2] M.Steck, K.Beckert, H.Eickhoff et al. Anomalous temperature reduction of electron-cooled heavy ion beams in the storage ring ESR. Phys.Rev.Lett., v.77 (1996) p.3803.
- [3] R.W.Hasse, M.Steck. Ordered ion beams. Proceeding of EPAC'2000.
- [4] H.Danared, A.Kallberg, K.G. Rensfelt, A.Simonsson. Observation of ordered ion beams in CRYRING. Proceeding of PAC'2001.
- [5] Kai Tezlaff. Diploma Thesis. Entwicklung einer Benutzeroberfläche für den TSR und Anwendungen im Bereich der Strahldiagnose. University of Heidelberg, 1997
- [6] I.Meshkov, A.Smirnov, A.Sidorin, J.Stein, J.Dietrich. Studies of beam dynamics in cooler rings. Proc. of COOL'05 Conference. Galena, USA, 2005.
- [7] T.Shirai et al. One dimensional beam ordering of protons in a storage ring, submitted to Phys. Rev. Lett.
- [8] <http://lepta.jinr.ru/betacool>
- [9] R.Hasse. Theoretical Verification of Coulomb Order of Ions in a Storage Ring. Phys. Rev. Letters, v.83, num.17. 25 October 1999.
- [10] M. Steck, P. Beller, K. Beckert, B. Franzke, F. Nolden. Electron cooling experiments at the ESR. NIM, A 532 (2004) 357–365
- [11] L. Michelotti. Intermediate Classical Dynamics with Application to Beam Physics. Wiley, New York 1995.
- [12] I.Meshkov. Electron beam for suppression of heavy ion oscillation at storage rings. Doctor Thesis. INP, Novosibirsk, 1975.
- [13] H. Danared, G. Andler, L. Bagge, A. K'allberg, F. Osterdahl, A. Pa'al, A. Simonsson, M. Ugglas. Studies of transverse electron cooling. Proceedings of EPAC 2000, Vienna, Austria.
- [14] V.Parkhomchuk, New insights in the theory of electron cooling, NIM A 441 (2000) 9-17, p.9
- [15] I.Meshkov, A.Sidorin, A.Smirnov, E.Syresin, T.Katayama, H.Tsutsui, D.Möhl. Simulation study of ordered ion beams. ISSN 1346-2431, RIKEN-AF-AC-42. July 2003.